J Surfact Deterg
DOI 10.1007/s11743-016-1889-5

ORIGINAL ARTICLE

Surface Dilational Rheology, Foam, and Core Flow Properties of Alpha Olefin Sulfonate

Hongsheng Liu[1] · Peihui Han[1] · Gang Sun[1] · Feng Pan[1] · Bo Li[1] · Jingqin Wang[2] · Changsen Lv[1]

Received: 17 November 2015 / Accepted: 7 October 2016

Abstract The surface tension, surface dilational rheology, foaming and displacement flow properties of alpha olefin sulfonate (AOS) with inorganic salts were studied. The foam composite index (FCI), which reflects foaming capacity and foam stability, is used to evaluate foam properties. It is found that sodium and calcium salts can lead to decreases in AOS surface tension, critical micelle concentration, and molecular area at the gas–liquid interface. Sodium ions reduce the surface dilational viscoelasticity (E) and FCI of AOS, while calcium ions can enhance the E of AOS and make the FCI of AOS reach a maximum. In the solution containing calcium and sodium ions, the FCI of AOS is improved. Crude oil reduces the FCI of AOS. Injection pressure and displacing efficiency of AOS alternating carbon dioxide (CO_2) injection are higher than injections of water alternating with CO_2 or CO_2 alone in low permeability cores.

Keywords Alpha olefin sulfonate · Surface tension · Surface dilational viscoelasticity · Foam composite index · Low permeability cores

Introduction

Foam is a dispersion of a gas phase in a continuous liquid phase, stabilized by surfactants and/or nano-particles [1, 2]. In the petroleum industry, foam can improve water or gas flooding by decreasing the mobility of the displacing fluids in reservoirs [3–5]. Foam generation is achieved either by co-injection of gas and surfactant into reservoirs or by alternating injections of surfactant and gas [6–8]. Crude oil can be displaced by foam flooding in two ways. The first is to stabilize the displacing process by increasing the viscosity of the displacing phases and blocking higher permeability zones. The second is to reduce the capillary forces by reducing the oil/water interfacial tensions by the presence of surfactant [8, 9]. Foam has been widely applied in oil recovery development [10, 11].

To achieve good mobility control, it is crucial that foam retains its foaming capacity and foam stability under reservoirs conditions [8, 12]. Surfactant is a key influence on foam properties, so surfactant selection is very important. Alpha olefin sulfonate (AOS) has a good foaming capacity, foam stability, salt resistance, biodegradability, low toxicity, and good oil compatibility. AOS is then an excellent candidate for foam application in enhanced oil recovery (EOR) fields [13, 14].

Interfacial tension is an important performance indicator of a surfactant, as are dynamic interfacial response of balance disturbance [15–17]. Thus, interfacial dilational rheology is a key interfacial dynamic property, and it is an occurring microscopic relaxation process on both the interface and subinterface [18–20]. It can help to understand the micro-dynamic interfacial behavior of surfactant [21, 22]. Interfacial dilational rheology includes interfacial dilational viscoelasticity, interfacial dilational elasticity, interfacial dilational viscosity, phase angle, dynamic, and

✉ Hongsheng Liu
liuhs9902@163.com

[1] Exploration and Development Research Institute of Daqing Oilfield Company Ltd., 163712 Daqing, China

[2] Production and Engineering Research Institute of Daqing Oilfield Company Ltd., 163453 Daqing, China

Published online: 19 October 2016

equilibrium interfacial tension. These parameters can be measured by the droplet or bubble expansion methods [23–25], which are suitable for evaluating interfacial dynamic characteristics of an emulsion or foam.

Foam evaluation parameters include foaming capacity (especially the initial volume of foam generated) and foam stability [26–31]. Foaming capacity is the maximum foaming volume of a surfactant under prescribed conditions. Foam stability in this work is defined as the time of foam volume to decay to half of the maximum foaming volume. To understand the foaming capacity and stability, foam the interactions between interfaces in the films are evaluated [1, 26, 27]. Two mono-layers of adsorbed surfactant molecules, separated by an aqueous layer, help to stabilize the film. The stability and thickness of these films influence both initial volume and longer term stability.

The relationship between surface dilational rheology and foam stability has been a focus of research in recent years. It is commonly believed that surface dilational rheology plays an important role in foam stability [27–31]; However, no consensus on a specific mechanism has been reached. Fruhner reported that pure elastic adsorption layers were not able to stabilize foam lamellae [27]. Zhang and Yan reported that low frequency elasticity played a positive effect on foam stability for certain systems and experimental conditions [28, 29]. Wang and Zhao reported that high surface viscoelasticity was responsible for high foam stability [30, 31].

In this paper, studies were of surface tension and surface dilational rheology on AOS systems with added sodium and/or calcium ions. Surface dilational rheology was measured by the bubble expansion method. Foam composite index (FCI), a comprehensive combination of foaming capacity, foam stability, and decay process, is used to evaluate foam properties of AOS in electrolyte systems. Flow and displacing experiments of AOS by alternating injection in low permeability natural cores were also done. The research results will provide useful guidance for AOS applications in EOR fields.

Materials and Methods

Materials

Alpha olefin sulfonate (AOS) was purchased from Xi'an Sun-wind Chemical Industry Group Co., Ltd.. The alkyl chain length of this AOS is $C_{14}\sim C_{16}$, and the active content is 35 wt%, with the remainder as 35 wt% sodium chloride and 30 wt% water. AOS is composed of 70 wt% alkenyl sulfonate and 30 wt% hydroxyl sulfonate; the average molecular weight of AOS is approximately 315. Sodium chloride (CAS: 7647-14-5) and calcium chloride (CAS: 10043-52-4) were purchased from Beijing Heng Ye Zhong Yuan Chemical Co., Ltd.. Carbon dioxide gas was provided by Daqing Snow Dragon Gas Co., Ltd. The natural cores were provided by the Daqing Oilfield.

Methods

Surface Tension Measurements

Surface tension was measured by the bubble pressure method at 45 °C. Before the surface tension measurement, the bubble was equilibrated for at least 20 min. The surface tension apparatus was provided by I.T. Concept, France.

Surface Dilatational Rheology Measurements

The surface dilational rheology apparatus was also provided by I.T. Concept, France. When the surface area of a bubble is deformed by dilation, the resistance against the changes in area provokes its own elastic and viscous responses [32–34]. The dilational modulus in compression and expansion is defined by,

$$E = \frac{\mathrm{d}\gamma}{\frac{\mathrm{d}A}{A}} = \frac{\mathrm{d}\gamma}{\mathrm{d}\ln(A)}, \tag{1}$$

where γ is the interface tension and A is the interface area. In the oscillatory experiments conducted here, dilational viscoelasticity (E) is a complex quantity.

$$E = E' + iE'', \tag{2}$$

where E is the total modulus, E' is the real part (i.e. dilational elasticity), and E'' is the imaginary part (i.e. dilational viscosity). The total modulus represents a change in the energy of the system with a corresponding area change. The elastic component can be regarded as the energy stored in the system, and the viscous component can be regarded as the loss energy. The elastic and viscous modulus can also be expressed in terms of the total modulus, and phase angle (θ), as follows:

$$E' = |E|\cos(\theta), \tag{3}$$

$$E'' = |E|\sin(\theta). \tag{4}$$

The results of surface dilational rheology depend on parameters including bubble volume, amplitude, and frequency. In this work, the bubble volume was 3.5 mL and the amplitude of oscillation was 10 % of the bubble volume. The bubble was equilibrated for at least 20 min at 45 °C. The surface dilational moduli were determined with changes of surface tensions and interface area in bubble sinusoidal oscillation.

Foam Properties Measurements

Foaming capacity and foam stability were measured by a foam scanner, which was purchased from I.T. Concept, France. The surfactant solutions were equilibrated for at least 20 min at 45 °C. Foam was generated by blowing CO_2 through a porous media filter at the bottom of the surfactant solution. The pore diameter of porous media filter was 0.2 mm, and the volume of surfactant solution was 50 mL, and the gas flow rate of CO_2 was 30 mL/min. Five minutes after the gas injection, the largest foaming volume was deemed the foaming capacity. The time of foam volume decaying to half of the foaming capacity was described as the foam stability.

FCI is used to evaluate foam properties. A schematic illustration of foaming capacity and foam stability is presented in Fig. 1. The curve of foam volume attenuation is not a straight line. Curve shape depends on surfactant properties and is a reflection of foam properties. The function $F(x)$ describes the attenuation curve of foam volume. FCI is the shadow triangular area below the curve, and calculation formula for FCI is as follows:

$$\mathrm{FCI} = \int_{t_0}^{t} [F(x) - F(t)]. \tag{5}$$

The foaming capacity, foam stability and decay process can be reflected by the FCI at the same time.

Adsorption Measurements

The natural cores of the Daqing oilfield were washed out, dried, and then crushed to 50–100 mesh particles. The experiment was equilibrated for 24 h at 45 °C. Concentrations of AOS were measured by a two-phase titration method.

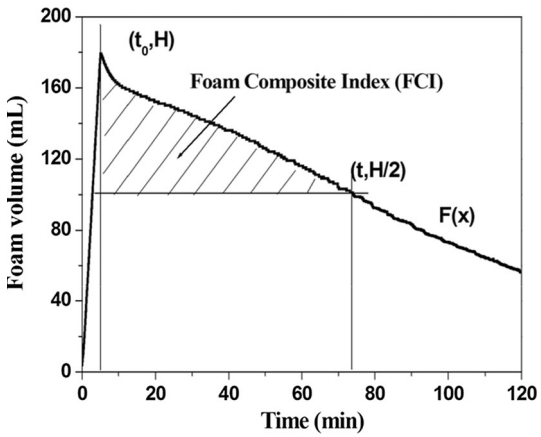

Fig. 1 Schematic illustration of foam formation and stability

Flow and Displacing Measurements

The instrument for flow and displacing experiment was provided by the Jiangsu Huaan Petroleum Apparatus Company. Experiment temperature was 45 °C. The size of natural cores was φ 2.5 cm × 12 cm, and gas permeability was about 0.07 μm^2. The cores were first put under a vacuum with a pump, and then saturated with water. The pore volume (PV) of the cores was calculated by measuring the amount of water required to saturate the core. AOS solutions and CO_2 as well as water and CO_2 were alternately injected into the cores, with the alternate cycle of 0.1 PV.

In flow experiments, the cores were first flooded by AOS alternating with CO_2, water alternating with CO_2, or CO_2alone, and then flooded by water until injection pressure remained stable. Injection pressure of the whole process *versus* the injected PV was recorded.

In displacing experiments, the cores were saturated with crude oil and aged for 24 h. The oil saturation of cores was calculated by measuring saturated crude oil and water volumes. The cores were first flooded by water, and then flooded by AOS alternating with CO_2, water alternating with CO_2, or CO_2 alone and finally, flooded by water. Injection pressure, oil and water production of the whole experiment process was recorded.

Results and Discussion

Surface Tension

The influences of inorganic salts on surface tension and critical micelle concentration (CMC) of AOS are presented in Fig. 2. The concentrations of sodium and calcium ions

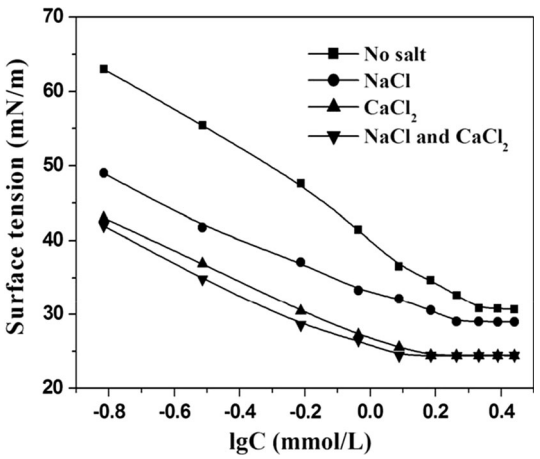

Fig. 2 The surface tension isotherms of AOS *versus* concentration of inorganic salts

are both 1.0 mmol/L, thus the total concentration of mixed sodium and calcium ions is 2.0 mmol/L. The surface tension of AOS reaches a minimum value at the concentration of 2.15 mmol/L. Inorganic salts lead to a decrease in surface tension and CMC of AOS. Calcium ions have an obviously stronger effect on AOS surface properties than sodium ions do. In the solution containing calcium and sodium ions, the reduction of surface tension is similar to that of calcium ions alone.

Farajzadeh. showed that the surface tension isotherms for different ionic strength coincide on a single curve, when plotted as a function of the mean ionic activity [13, 34]. The curves of AOS surface tension *versus* mean ionic activity are presented in Fig. 3. The surface tension isotherms of AOS with sodium and/or calcium chloride pass through a master curve without inorganic salts. This indicates that surface tension of AOS with the inorganic salts studied is independent of electrolyte concentration at a given mean ionic activity. The calculated adsorptions *versus* the mean ionic activity are presented in Fig. 4. The adsorption continuously increases with the addition of either inorganic salts or surfactant. Inorganic salts lead to an increase in AOS adsorption, and calcium ions have a stronger effect on the adsorption of AOS than sodium ions do. This can be attributed to enhanced electrostatic screening in the double layer and decreased repulsion.

The calculation method of Farajzadeh is used to analyze and understand the molecular arrangement of the surfactant at the gas–liquid surface [13]. The saturated absorption (Γ_m) is calculated, and the surfactant molecular area (A_m) is obtained at Γ_m. The molecular arrangement is speculated by analyzing the A_m of Γ_m [34]. The results calculated from data of Figs. 2 and 4 are presented in Table 1.

The A_m of AOS without added electrolyte at Γ_m is 0.53 nm^2 at the gas–liquid surface, which indicates that the

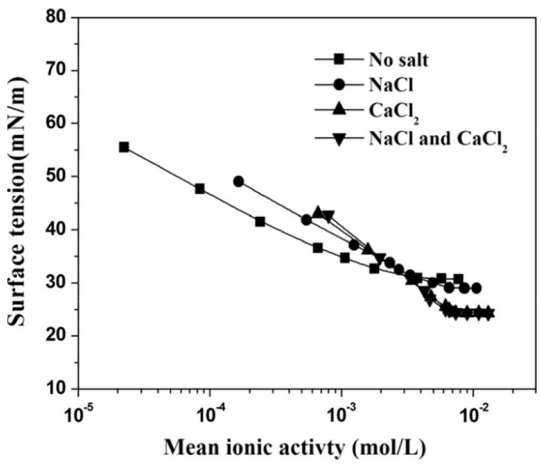

Fig. 3 The surface tension isotherms *versus* mean ionic activity for AOS solutions with different inorganic salts

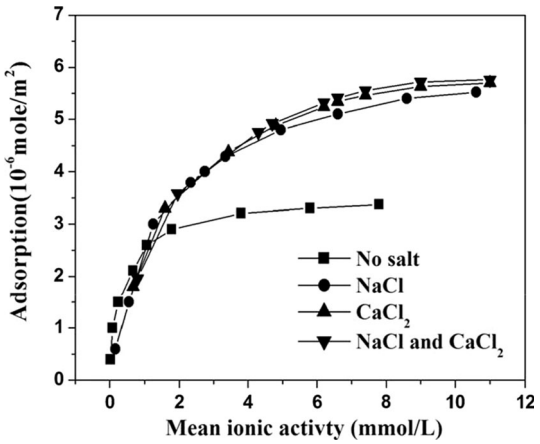

Fig. 4 Calculated adsorption *versus* mean ionic activity for AOS solutions with different inorganic salts

AOS molecular arrangement is not close. This is because of the hydration and electrostatic effects of the AOS molecular hydrophilic group. The alkenyl and hydroxyl groups, which bend AOS molecules, do not meet in a side by side vertical arrangement, thus the surface tension of AOS is higher. Inorganic salts decrease A_m of AOS at Γ_m at the gas–liquid surface, thus AOS molecular arrangement becomes closer. Due to the calcium or sodium ions compressing the double layer of AOS ions, the repulsion force of AOS intermolecular is reduced. The AOS molecular arrangement is more vertical at the gas–liquid surface and favorable to the formation of micelles.

Calcium ions reduce hydration of AOS more easily than sodium ions do. In the solution containing calcium and sodium ions, calcium ions play a leading role. AOS molecular arrangement becomes more upright and closely packed, and the A_m of AOS at Γ_m is only about 0.29 nm^2 in the solution containing calcium ions.

Surface Dilational Rheology

The effect of working frequency on surface dilational rheology of AOS is presented in Fig. 5. Surface dilational viscoelasticity (E), surface dilational elasticity (E'), and surface dilational viscosity (E'') of AOS increase with increasing working frequency. As the working frequency increases, recovery time is reduced for adsorption of AOS molecule at the gas–liquid surface by a diffusion-exchange relaxation process, thus restoration of surface tension gradients caused by surface deformation is incomplete.

Surface dilational moduli of AOS *versus* concentration are presented in Fig. 6. The E of AOS increases with concentration, reaches a maximum at a concentration of 0.07 mmol/L, then reduces as concentration continues to increase, and finally stabilizes. The E value of AOS is greater than 10 mN/m, which indicates that AOS surface

Table 1 The adsorption parameters AOS with different inorganic salts

Salt type	C_{salt} (mmol/L)	C_{CMC} (mmol/L)	γ_{CMC} (mN/m)	Γ_m (10^{-6} mol/m^2)	A_m (nm^2)
No salt	0.0	2.15	30.89	3.12	0.53
NaCl	1.0	1.84	29.05	5.25	0.32
$CaCl_2$	1.0	1.53	24.45	5.61	0.30
NaCl and $CaCl_2$	2.0	1.22	24.41	5.75	0.29

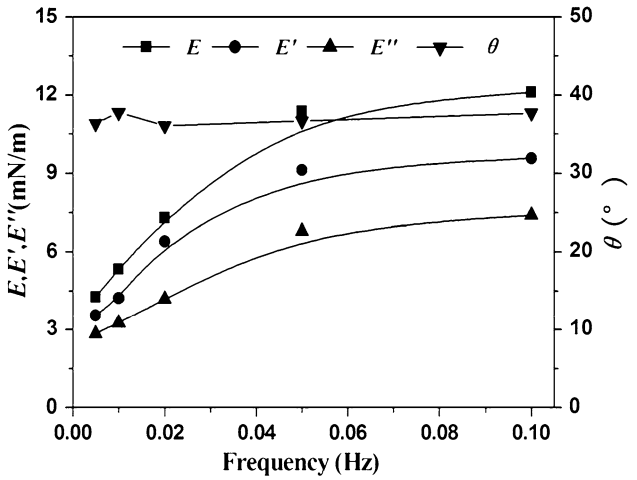

Fig. 5 The surface dilational rheology of AOS *versus* working frequency

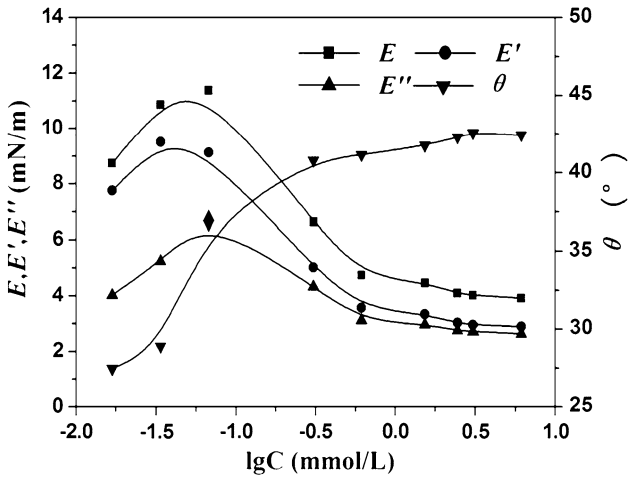

Fig. 6 The surface dilational rheology of AOS *versus* concentration

dilational rheology is strong. The phase angle of AOS gradually increases with concentration, but it is always less than 45°. This indicates that E is dominated by E' (elasticity) and not viscosity. When the surface shape is changed in the entire range of concentration, E' of AOS is always stronger than E''.

The Tempel–Lucassen model explains the relationship between concentration and surface dilational rheology [35]. When the AOS concentration is below the CMC, increased AOS concentration has two influences on surface dilational rheology. On the one hand, surface adsorption of AOS molecules is increased. When the surface shape is changed, a high surface tension gradient is obtained, resulting in a higher E. On the other hand, diffusion and supplement of AOS molecules from the solution phase to newly generated surface is imposed. The diffusion of AOS molecules to the surface is mainly controlled by the following factors, such as AOS molecular structure, concentration difference of the surface phase and solution phase, and so on. The ability of diffusion and the supplement can eliminate the surface tension gradient, so it reduces E.

Increasing surface adsorption plays a dominant role at low concentrations, so E increases. As the concentration further increases, the function of diffusion and the supplement is dominant, and the E decreases. In the vicinity of the CMC of AOS, the function of diffusion and supplement has a significant increase, and the trend of E reduction is more obvious. There is a maximum value of E as the AOS concentration increases.

Effect of Inorganic Salts on Surface Dilational Rheology

The effect of sodium ions on the surface dilational rheology of AOS is presented in Fig. 7. (AOS concentration is 0.07 mmol/L in this set of experiments.) Sodium ions reduce E of AOS. When sodium ions concentration is more

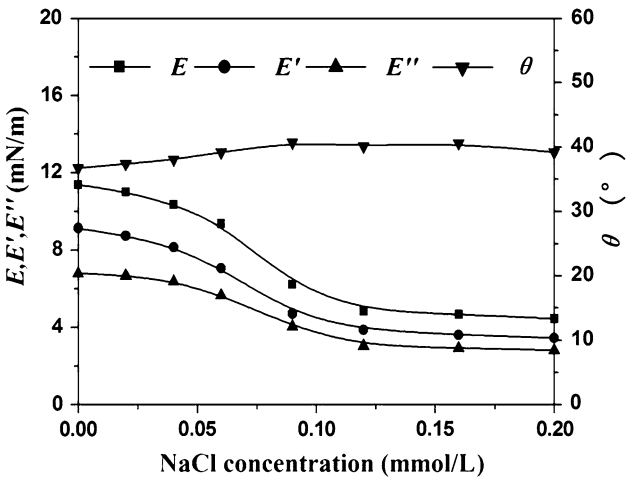

Fig. 7 The surface dilational rheology of AOS *versus* sodium ions concentration

than 1.2 mmol/L, the E of AOS tends to stable. But the E value of AOS is very low, and the phase angle of AOS does not change significantly.

Sodium ions compress the double layer of AOS ions, thus intermolecular repulsion of AOS is weakened, the surface tension and the CMC of AOS are reduced, and the AOS molecular arrangement is more upright and close in the surface film. Schematic illustration of AOS and sodium ions in the surface film is presented in Fig. 10. When a deformation occurs in the surface film, diffusion and supplement of AOS molecules from solutions to a new generated surface film is strengthened by sodium ions. The E' of AOS thus decreases. Sodium ions make the relaxation processes relatively easy, which are molecular exchange in the surface phase and solutions phase, molecular arrangement and change in the surface, and so on. The E'' of AOS then decreases. Thus E of AOS is reduced. The effect of sodium ions on E' of AOS is larger than on E''. Therefore, the phase angle slightly increases.

The effect of calcium ions on the surface dilational rheology of AOS is presented in Fig. 8. When calcium ions concentration is very low, the E of AOS reaches maximum value. When calcium ions concentration is more than 0.06 mmol/L, the E of AOS is reduced, and finally stabilized. The E' value of AOS is greater than E'' at dilational modulus peak. Thus the phase angle of AOS is reduced to a minimum. As the calcium ions concentration increases, the difference in E' and E'' diminishes. Thus the phase angle of AOS slowly increases, but remains below 45°.

The alkenyl group, hydroxyl group and sulfonic group of AOS form stable ionic groups, and the removal of hydration of the sulfonic group is more difficult. Therefore inorganic salts ions are hard to reach the hydration layer of AOS ions. AOS and sodium ions or calcium ions cannot form precipitates. When calcium ions concentration is very low, two or more AOS molecules can bind with one calcium ion at the same time. When a deformation occurs in surface film, AOS molecules do not easily spread to the new surface due to the binding effect of AOS and calcium ions in solution phase. The repulsion among AOS molecules is reduced in the gas–liquid surface arrangement. Thus E' of AOS increases. Schematic illustration of AOS and calcium ions in surface film is presented in Fig. 10. The relaxation processes become relatively difficult, which includes molecular exchange in the surface and solution phase, molecular arrangement and change in the surface, and so on. Therefore, the E'' of AOS increases. When calcium ions concentration is increased, the case that two or more AOS molecules binding with one calcium ion is significantly reduced, and one AOS molecules binding with one or more of calcium ions is mainly formed. At this time, the E of AOS decreases.

The hydration removal and interaction of AOS molecules with calcium ions are stronger than those of sodium ions at the same concentration. In the solution containing calcium and sodium ions, calcium ions plays a dominant role. Therefore, the E changing trend of AOS is the same as that of single calcium ions (Figs. 9, 10).

Effect of Inorganic Salts on Foam Properties

The foam properties of AOS *versus* concentration are presented in Fig. 11. The FCI of AOS increases quickly with concentration, reaching a maximum at about 3.0 mmol/L, and then slowly reduces. When AOS concentration is above 2.5 mmol/L, the foam volume is close to the gas volume used for foaming. This indicates that AOS foaming capacity reaches a maximum.

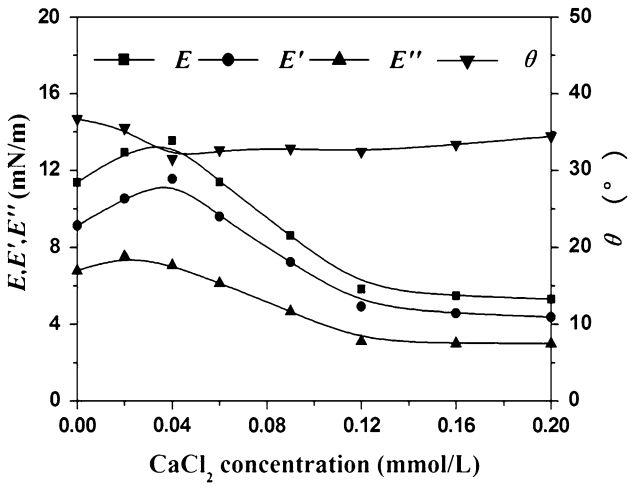

Fig. 8 The surface dilational rheology of AOS *versus* calcium ion concentration

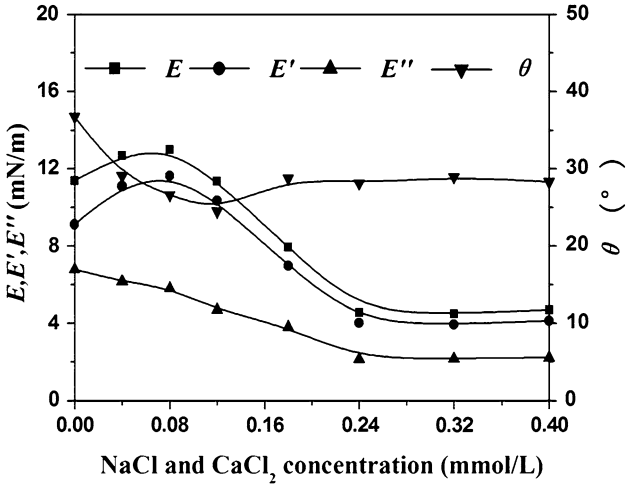

Fig. 9 The surface dilational rheology of AOS *versus* sodium and calcium ions concentration

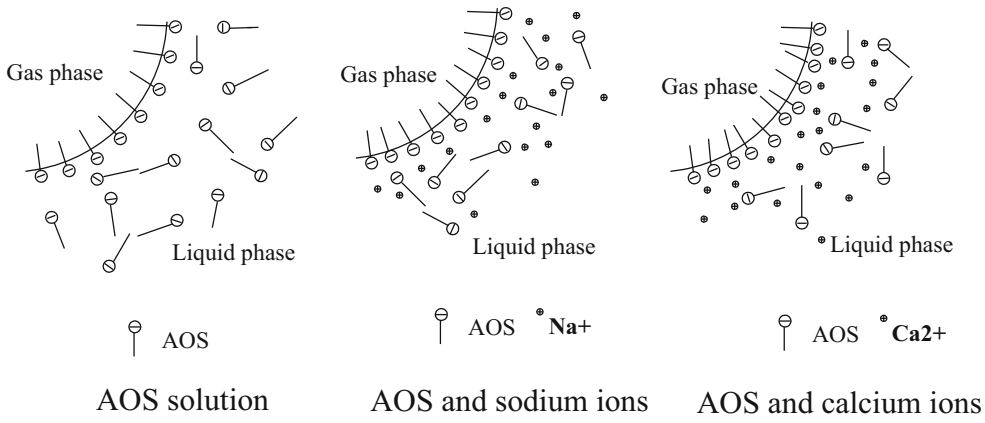

Fig. 10 Schematic illustration of AOS with inorganic salts in the surface film

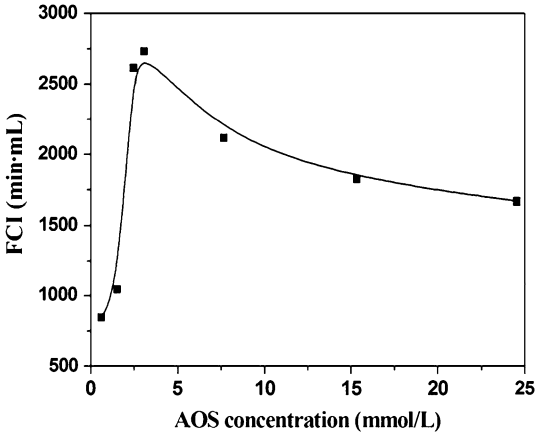

Fig. 11 The FCI of AOS *versus* concentration

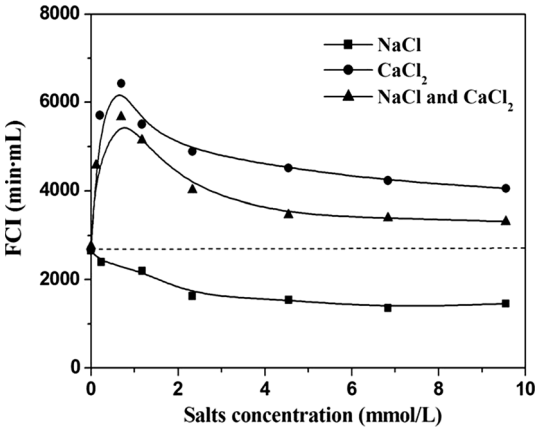

Fig. 12 The FCI of AOS *versus* different inorganic salts concentration

The effect of inorganic salts on FCI of AOS is presented in Fig. 12. The concentration of AOS is 3.0 mmol/L. Sodium ions reduce FCI of AOS, while calcium ions increase FCI of AOS in low concentration. As calcium ions concentration increase, FCI of AOS tends to stabilize, at a high value. The foam volume of different systems makes no difference, so the difference of FCI is primarily caused by foam stability.

There are many influential factors on foam stability, such as surface tension, adsorption, surface dilational rheology, solution viscosity, ionic strength, temperature, and foaming method [36–38]. In this paper, experimental conditions of solution viscosity, temperature, and foaming method are the same. Therefore, the primary influencing factors on foam are surface tension, adsorption, ionic strength, and surface dilational rheology.

The influence of ionic strength on adsorption of AOS is similar with the presence of calcium ions or mixed sodium and calcium ions, but their influence on surface dilational rheology in the low AOS concentration regime is different. Calcium ions may form complexes with two AOS molecules simultaneously. Low frequency measurement of surface dilational rheology provides evidence for the changes of adsorption and surface layer rearrangement in region of low AOS concentration. At high concentration, the accuracy of this method is not sufficient, but the study results of Noskov showed that high frequency surface dilational rheology was strongly dependent on the relaxation time of surfactant micelle, which was influenced by calcium ions [39, 40]. Moreover, Shah demonstrated a strong correlation between foam stability and micelle relaxation time [41]. Thus, increased surface dilational rheology at low AOS concentration and increased foam stability at high AOS concentration in the presence of calcium ions have the same causes.

Effect of Oil on Foam Properties

The effect of crude oil on AOS foam properties is presented in Fig. 13. The AOS concentration in this experiment is 3.0 mmol/L, and sodium and calcium ions are respectively 1.0 mmol/L. Crude oil clearly reduces the FCI of AOS. As the content of crude oil increases, the FCI continues to reduce, and eventually remains at a low value.

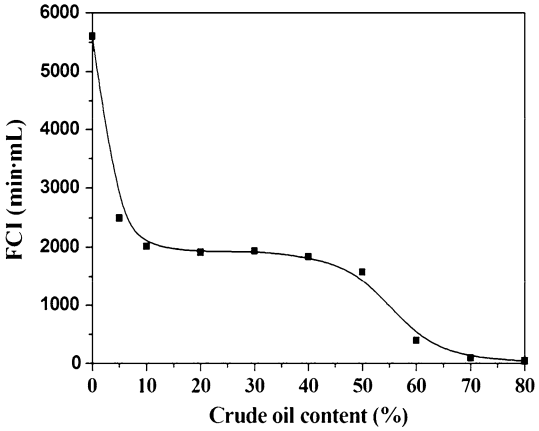

Fig. 13 The FCI of AOS *versus* crude oil content

When the crude oil content is more than 50 %, the FCI reduces again. The FCI decreases to zero in crude oil content over 70 %. The effect of crude oil on FCI is mainly due to two reasons. One reason is the partitioning of AOS to solubilize crude oil, and the other reason is the impact of crude oil on foam stability.

Adsorption Properties

Adsorption is the main factor for loss of AOS in reservoirs. The adsorption quantity of AOS on sands is presented in Fig. 14. With AOS concentration increasing, the adsorption quantity on sands increases. When AOS concentration exceeds 45 mmol/L, the adsorption capacity tends to stabilize, and the adsorption quantity is 8 mmol/g at equilibrium. Due to the clay contained in the sands, lots of AOS molecules are adsorbed, resulting in the larger adsorption quantity of AOS at equilibrium.

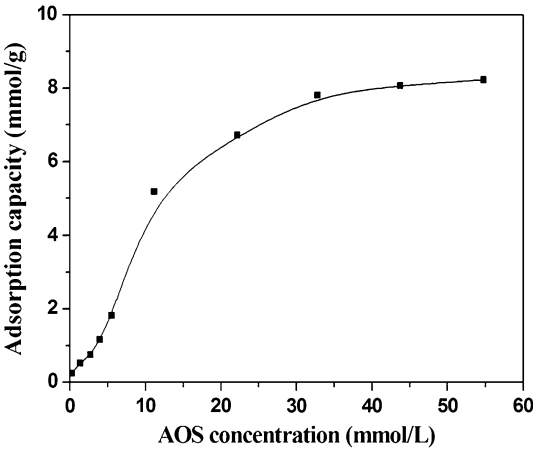

Fig. 14 The adsorption isotherms of AOS *versus* concentration

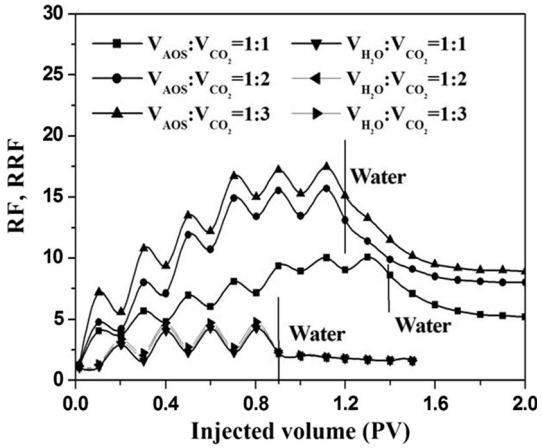

Fig. 15 The RF (before final water injection) and RRF (after final water injection) of AOS alternating CO_2 and water alternating CO_2 *versus* injected volume

Flow Properties

Resistance factors (RF, the ratio of mobility of the water to that of the treatment (surfactant solution or CO_2)) and residual resistance factors (RRF, the ratio of permeability of water before treatment to the water permeability after treatment) of AOS alternating CO_2 and water alternating CO_2 are presented in Fig. 15. AOS concentration is 3.0 mmol/L, and sodium and calcium ions are respectively 1.0 mmol/L. The RF of AOS alternating CO_2 injection is clearly higher than those of water alternating CO_2. At different gas:liquid ratios, the RF of AOS alternating CO_2 injection is greatly different from those of water alternating CO_2. The RF of AOS alternating CO_2 injection increases as the gas:liquid ratio increases. The trend of RRF change is the same as that of RF.

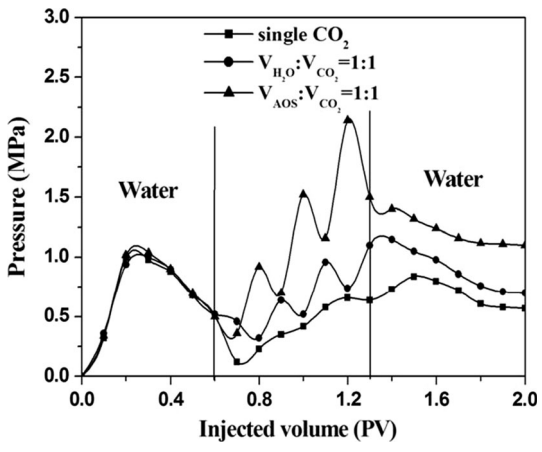

Fig. 16 The injection pressure of different displacing methods *versus* injected volume

Table 2 The cores displacing results of different displacing methods

Core #	Core length (cm)	Gas permeability ($10^{-3}\mu m^2$)	Oil saturation (%)	Water flooding EOR (%)	Liquid alternating gas flooding EOR (%)	Total EOR (%)	Gas liquid ratio
1	7.8	70.5	62.5	36.4	18.5	54.9	CO_2:AOS = 3:1
2	8.7	65.1	62.8	36.8	17.9	54.6	CO_2:AOS = 2:1
3	6.4	78.5	63.3	37.2	16.1	53.3	CO_2:AOS = 1:1
4	8.6	72.3	62.2	37.1	12.8	49.9	CO_2:H_2O = 3:1
5	8.2	68.5	62.4	36.9	12.3	49.2	CO_2:H_2O = 2:1
6	7.8	79.5	63.1	37.2	11.6	48.8	CO_2:H_2O = 1:1
7	7.9	62.6	62.6	36.4	6.8	43.2	Single CO_2

Water alternating CO_2 injection does not produce foam in cores, but this injection procedure can improve the sweep volume of gas to some extent. While AOS alternating CO_2 injection can produce foam, and the foam can increase CO_2 gas viscosity and block higher permeability zones. Thus the RF of AOS alternating CO_2 injection is higher than water alternating CO_2. With the gas liquid ratio increasing, gas content increases in porous media of cores, and more foam is generated in porous media, which helps to plug larger pores in cores, and adjust core permeability. Therefore, the RF of AOS alternating CO_2 injection increases.

Displacing Properties

The injection pressure of different displacing methods *versus* injected volume is presented in Fig. 16. AOS concentration is 3.0 mmol/L, and sodium and calcium ions are respectively 1.0 mmol/L. Injection pressures of initial water flooding in different cores are comparable. Injection pressure of AOS alternating CO_2 flooding is higher than those of water alternating CO_2, and the single CO_2. Injection pressure of AOS alternating CO_2 flooding is higher than that of the water flooding, and injection pressures of subsequent water flooding is also at a high value. Foam has been formed after AOS alternating CO_2 flooding in cores, and larger pores are effectively plugged by foam, which results in enlarged swept volumes and improved recovery factor.

The cores displacing results of different injection methods are presented in Table 2. Recovery efficiency of AOS alternating CO_2 flooding is higher than those of water alternating CO_2, and the single CO_2. The way of AOS alternating CO_2 flooding can improve oil recovery efficiency by 16–19 %, which is 6 % higher than those of water alternating CO_2, and is 10 % higher than that of the single CO_2. The oil recovery efficiency of AOS alternating CO_2 flooding increases with the gas liquid ratio. Total oil recovery efficiency of cores is more than 50 %. As the foam can effectively block the high-permeability pores and enlarge sweeping volumes, it can move forward in cores homogeneously [12, 42]. Meanwhile, AOS can decrease interface tension of crude oil, and improve displacing efficiency to a certain extent. Eventually, the AOS alternating CO_2 flooding improves oil recovery efficiency by more than 16 %.

Conclusions

Calcium ions have a stronger effect on the surface properties of AOS than sodium ions do. In the solution containing calcium and sodium ions, the function of calcium ions is more significant. The E' of AOS is greater than E'', indicating that elasticity dominates over viscosity in the surface dilational rheology. Sodium ions can reduce the E and FCI of AOS, while calcium ions can enhance the E of AOS and make the FCI of AOS reach a maximum. In the solution containing calcium and sodium ions, the FCI of AOS can be improved. Crude oil reduces the FCI of AOS. Injection pressure and displacing efficiency of AOS alternating with CO_2 flooding are higher than those of water alternating with CO_2, and the CO_2alone in low permeability cores. AOS alternating CO_2 flooding can improve oil recovery efficiency by more than 16 % after water flooding in low permeability cores.

Acknowledgments The authors are grateful for the financial support of the Major Project of Chinese National Ministry of Science and Technology Major Projects of China (Grant Number: 2011ZX05010).

References

1. Exerowa D, Kruglyakov PM (1998) Foam and foam films: theory, experiment, application. Elsevier, New York
2. Binks BP, Horozov TS (2005) Aqueous foams stabilized solely by silica nanoparticles. Ang Chem Int Ed 44(24):3722–3725
3. Boud DC, Holbrook OC (1958) Gas drive oil recovery process. US patent 2866507

4. Craig Jr FF, Lummus JL (1965) Oil recovery by foam drive. US patent 3185634
5. Holm LW (1968) The mechanism of gas and liquid flow through porous media in the presence of foam. Soc Pet Eng J 8(4):359–369
6. Du DX, Beni AN, Farajzadeh R, Zitha PLJ (2008) Effect of water solubility on carbon dioxide foam flow in porous media: an X-ray computed tomography study. J Ind Eng Chem 47(16): 6298–6306
7. Du D, Zitha PLJ, Uijttenhout MGH (2007) Carbon dioxide foam rheology in porous media: a CT scan study. SPE J 12(2):245–252
8. Farajzadeh R, Andrianov A, Krastev R, Hirasaki GJ, Rossen WR (2012) Foam–oil interaction in porous media: implications for foam assisted enhanced oil recovery. Adv Colloid Interface Sci 183–184:1–13
9. Al-Attar HH (2011) Evaluation of oil foam as a displacing phase to improve oil recovery: a laboratory study. J Pet Sci Eng 79(3):101–112
10. Skauge A, Aarra MG, Surguchev L, Martinsen HA, Rasmussen L (2002) Foam-assisted WAG: experience from the Snorre field. SPE/DOE Improved Oil Recovery Symposium, 13–17 April 2002, Tulsa, Oklahoma; SPE 75157
11. Jongh CD, Lund E, Hole M, Duncan J (2007) Ula WAG-world class EOR-breathing the gas of life into a mature oil field. IOR 2007—14th European Symposium on Improved Oil Recovery
12. Mannhardt K, Novosad JJ, Schramm LL (1998) Foam/oil interactions at reservoir conditions. SPE/DOE Improved Oil Recovery Symposium, 19–22 April, Tulsa, Oklahoma SPE 39681
13. Farajzadeh R, Krastev R, Zitha PLJ (2008) Foam films stabilized with alpha olefin sulfonate (AOS). Colloids Surf A 324(1–3):35–40
14. Simjoo M, Rezaei T, Andrianov A, Zitha PLJ (2013) Foam stability in the presence of oil: effect of surfactant concentration and oil type. Colloids Surf 438(45):148–158
15. Jing ZS (1999) Conspectus of surfactant. China national light industry publishing company, Beijing
16. Dollet B, Aubouy M, Graner F (2005) Anti-inertial lift in foams: a signature of the elasticity of complex fluids. Phys Rev Lett 95:168303
17. Kruglyakov PM, Elaneva SI, Vilkova NG (2011) About mechanism of foam stabilization by solid particles. Adv Colloid Int Sci 165:108–116
18. Rosen MJ, Hua XYJ (1982) Surface concentrations and molecular interactions in binary mixtures of surfactants. J Colloid Interface Sci 86:164–172
19. Pandey S, Bagwe RP, Shah DO (2003) Effect of counterions on surface and foaming properties of dodecyl sulfate. J Colloid Interface Sci 267:160–166
20. Theander K, Pugh RJ (2003) Synergism and foaming properties in mixed nonionic/fatty acid soap surfactant systems. J Colloid Interface Sci 267:9–17
21. Fruhner H, Wantke K-D, Lunkenheimer K (1999) Relationship between surface dilational properties and foam stability. Colloids Surf A 162:193–202
22. Bhattacharyya A, Monroy F, Langevin D, Argillier JF (2000) Surface rheology and foam stability of mixed surfactant-polyelectrolyte solutions. Langmuir 16:8727–8732
23. Ravera F, Loglio G, Pandolfini P, Santini E, Liggieri L (2010) Determination of the dilational viscoelasticity by the oscillating drop/bubble method in a capillary pressure tensiometer. Colloids Surf A 365(1–3):2–13
24. Del Gaudio LD, Pandolfini P, Ravera F, Krägel J, Santini E, Makievski AV, Noskov BA, Liggieri L, Miller R, Loglio G (2008) Dynamic interfacial properties of drops relevant to W/O-emulsion-forming systems: a refined measurement apparatus. Colloids Surf A 323(1):3–11
25. Fainerman VB, Zholob SA, Petkov JT, Miller R (2008) $C_{14}EO_8$, adsorption characteristics studied by drop and bubble profile tensiometry. Colloids Surf A 323(1–3):56–62
26. Alahverdjieva VS, Khristov K, Exerowa D, Miller R (2008) Correlation between adsorption isotherms, thin liquid films and foam properties of protein/surfactant mixtures: lysozyme/C_{10}-DMPO and lysozyme/SDS. Colloids Surf A 323(1–3):132–138
27. Fruhner H, Wantke K-D, Lunkenheimer K (2000) Relationship between surface dilational properties and foam stability. Colloids Surf A 162(1–3):193–202
28. Zhang H, Xu G, Liu T, Xu L, Zhou Y (2013) Foam and interfacial properties of tween 20–bovine serum albumin systems. Colloids Surf A 416(416):23–31
29. Yan F, Zhang L, Zhao RH, Huang HY, Dong LF, Zhang L (2012) Surface dilational rheological and foam properties of aromatic side chained n-acyltaurate amphiphiles. Colloids Surf A 396(7):317–327
30. Wang J, Nguyen AV, Farrokhpay S (2016) Effects of surface rheology and surface potential on foam stability. Colloids Surf A 488:70–81
31. Zhou ZH, Zhang L, Xu ZC, Zhang L, Zhao S, Yu JY (2011) Surface dilational properties and foam properties of novel benzene sulfonate surfactants. J Dispers Sci Tech 32:95–101
32. van den Tempel M, Lucassen-Reynders EH (1983) Relaxation processes at fluid interfaces. Adv Colloid Interface Int Sci 18(3–4):281–301
33. Lucassen-Reynders EH (1981) Surface elasticity and viscosity in compression/dilation in anionic surfactants. In: Lucassen-Reynders EH (ed) Anionic surfactants: physical chemistry of surfactant action. Marcel Dekker, Inc, New York
34. Zhao GX, Zhu BY (2003) Principles of surfactant action. China Light Industry Press, Beijing
35. Lucassen J, van den Tempel M (1972) Longitudinal waves on visco-elastic surfaces. J Colloid Interface Sci 41(3):491–498
36. Murray BS, Ettelaie R (2004) Foam stability: proteins and nanoparticles. Curr Opin Colloid Interface Sci 9(5):314–320
37. Tan SN, Fornasiero D, Sedev R, Ralston J (2005) The role of surfactant structure on foam behaviour. Colloid Surf A 263(1–3):233–238
38. Grassia P, Neethling SJ, Cervantes C, Lee HT (2006) The growth, drainage and bursting of foams. Colloid Surf A 274(1–3):110–124
39. Noskov BA, Loglio G (1998) Dynamic surface elasticity of surfactant solutions. Colloid Surf A 143(2–3):167–183
40. Noskov BA (2002) Kinetics of adsorption from micellar solutions. Adv Colloid Interface Sci 95(2–3):237–293
41. Patist A, Kanicky JR, Shukla PK, Shah DO (2002) Importance of micellar kinetics in relation to technological processes. J Colloid Interface Sci 245(1):1–15
42. Farajzadeh R, Muruganathan RM, Rossen WR, Krastev R (2011) Effect of gas type on foam film permeability and its implications for foam flow in porous media. Adv Coll Interface Sci 168(1–2):71–78

Hongsheng Liu obtained his master's degree from the China University of Petroleum-Beijing in China. His research deals with interface property and chemical flooding.

Peihui Han received his Ph.D. from the China University of Geosciences-Beijing in China. His research deals with foam property and chemical flooding.

Gang Sun is an undergraduate at the Heilongjiang University in China. His research deals with chemical flooding.

Feng Pan is an undergraduate at the Wuhan University in China. His research deals with chemical flooding.

Bo Li obtained his master's degree from the Central South University in China. His research deals with interface property.

Jingqin Wang obtained her master's degree from the Liaoning Shihua University in China. Her research deals with foam property.

Changsen Lv obtained his master's degree from the Daqing Petroleum Institute in China. His research deals with interface property.